Nuclear Engineering and Technology 56 (2024) 1425–1430

Contents lists available at ScienceDirect

Nuclear Engineering and Technology

journal homepage: www.elsevier.com/locate/net

Original Article

Fabrication of a superheated emulsion based on Freon-12 and LiCl suitable for thermal neutrons detection

Sara Sadat Madani Kouchak [a], Dariush Rezaei Ochbelagh [a,*], Peiman Rezaeian [b], Majid Abdouss [c]

[a] Department of Physics and Energy Engineering, Amirkabir University of Technology, Tehran, Iran
[b] Radiation Applications Research School, Nuclear Science and Technology Research Institute, AEOI, Tehran, Iran
[c] Department of Chemistry, Amirkabir University of Technology, Tehran, Iran

ARTICLE INFO

Keywords:
Superheated emulsion detector
Thermal neutron
Freon-12

ABSTRACT

This study develops superheated emulsion detectors that are both sensitive to fast neutrons, and thermal neutrons owing to the exergonic ${}^{6}_{3}Li(n,\alpha)^{3}_{1}H$ capture reaction caused by the ^{6}Li-containing compound dispersed throughout the gel-like medium. The experimental research was conducted on two SEDs. One detector was an ordinary Freon-12 detector and the other was a Freon-12 detector containing 3.4 % (by weight) LiCl. In order to investigate the sensitivity of lithium-containing SEDs to thermal neutrons, two types of SEDs were simultaneously exposed to various flux levels of thermal neutrons from ^{241}Am–Be neutron source inside a cylindrical tank filled with water. A Boron-lined proportional counter was used to estimate the thermal neutron flux and the relevant MCNP code was developed for flux and dose calculations in the prepared set-up around ^{241}Am–Be source. The results demonstrate that there is a proportional relationship between the variations of SED response and the change in thermal neutron flux and dose. Also, the sensitivity of SED was estimated.

1. Introduction

Thermal neutrons have gained a wide range of applications in various fields such as medicine [1], crystallography [2], and homeland security [3]. There are several detectors to detect thermal neutrons such as ^{3}He gas counters, BF_3 detectors Boron-lined detectors, and lithium scintillation detectors. Due to its low toxicity, high pulse resolution, insensitivity to gamma radiation, and physical robustness, the ^{3}He gas counter is typically the preferred choice for thermal neutron fields over other neutron detectors [4–6]. However, the lack of ^{3}He in the world [7] has made the use of other neutron detectors in different fields necessary.

Superheated emulsion detectors (SED) are metastable suspensions of minute droplets of superheated liquids in a viscoelastic gel (superheated droplet detector, SDD) [8] or in a polymer medium (bubble detector, BD) [9] that readily vaporize into bubbles when affected by nuclear radiation interactions. Some advantages of SED include direct reading capability, passive operation, insensitivity to γ-rays [9], and ease of use without requiring a power supply [10]. SEDs are mainly used for fast neutron detection because their efficiency for thermal neutrons is low. In order to monitor and determine the dose of thermal neutrons, Bubble Technology Industries introduced the bubble neutron dosimeter model BDT. BDT consists of a plastic tube that contains thousands of superheated liquid drops of Freon-12 (CCl_2F_2, boiling point $-29.8\ ^{\circ}C$ at atmospheric pressure) [11] dispersed in a firm polymer medium containing Li. Among all the superheated liquids studied so far, Freon-12 possesses some, albeit small, sensitivity to thermal neutrons at ambient temperature and pressure due to the exoergic ${}^{35}_{17}Cl(n,p)^{35}_{16}S$ capture reaction (with the cross-section 0.489 b for 25.3 meV neutrons) [12–14]. Therefore, adding Li (with the cross-section 940 barns for thermal neutrons) leads to the increased sensitivity of detectors to thermal neutrons.

As a further comparison BDT is a good commercial dosimeter with its specific shape and dimensions, while SED can be manufactured in various sizes and shapes to accommodate specific requirements.

In this study, first we analyze, by theory and via utilizing the stopping power of lithium and thermal neutron interaction products, how the presence of lithium in the gel medium affects the bubble formation. In the experimental research, to evaluate the thermal neutron sensitivity of SED, the ordinary Freon-12 detector and the Freon-12 detector based on ^{6}Li were exposed simultaneously to a thermal neutron field at various distances. Then the bubbles were counted visually. Fast neutrons result in bubbles to be formed in ordinary Freon-12 detectors while the

* Corresponding author.
E-mail address: ddrezaey@aut.ac.ir (D. Rezaei Ochbelagh).

https://doi.org/10.1016/j.net.2023.11.046
Received 10 June 2023; Received in revised form 19 November 2023; Accepted 27 November 2023
Available online 11 December 2023

thermal neutrons contribute to the difference in the number of formed bubbles in the two types of SED. In addition, the average neutron flux was determined by the MCNP code and the Boron-lined proportional counter. Afterwards, the relation between the response of the SED and the thermal neutron flux was examined in the prepared set-up. Finally, utilizing the dose obtained from the MCNP code, the SED's Sensitivity (bubble/μSv) was estimated according to the NCRP-38 recommendations. It is noteworthy that the strength of the polymer medium affected the rate of bubble formation [15]. Since the process of bubble formation in the gel is faster than that in a firm polymer, the gel was used as the host medium in the present work [16]. The gel medium enables the fabrication of detectors in various dimensions tailored for specific purposes.

2. Theory

When a SED is exposed to a neutron field, droplets of superheated liquid dispersed in a viscoelastic gel turn into bubbles. A linear relationship exists between the neutron flux and the number of nucleated bubbles [17]. The Seitz theory describes the SED bubble formation process [18], which explains that recoil ions from elastic scattering interactions transfer kinetic energy to superheated droplets suspended in a gel. Recoil ions passing through superheated droplets deposit energy along their path, generating microbubbles. Equation (1) expresses the minimum amount of energy required to transform a microbubble into a visible bubble [8].

$$W = 16\pi\gamma^3(T) \,/\, 3(P_v - P_o)^2 \tag{1}$$

Here, $\gamma(T)$ and P_v and P_o represent the superheated liquid's surface tension at temperature T, the superheated liquid's vapor pressure, and the external pressure applied to the surface of the viscoelastic gel, respectively. As microbubbles expand to the critical radius (r_c), they become thermodynamically unstable and grow rapidly until the whole liquid droplet vaporizes into a visible bubble. If the microbubbles have not reached the critical radius, then the microbubbles will be compressed under the surface tension and pressure of the medium. The critical radius (r_c), is given by Ref. [8]:

$$r_c = 2\gamma(T) \,/\, (P_v - P_o) \tag{2}$$

A recoiled ion's deposited energy is proportional to its stopping power (dE/dx). Only a small percentage of the energy deposited by the recoil ion at a distance of $2r_c$ contributes to nucleation [19], as defined by the thermodynamic efficiency of nucleation (η). Therefore, the condition for bubble formation is:

$$\eta(2r_c)\left(\frac{dE}{dx}\right) \geq W \tag{3}$$

By inserting Eq. (1) and Eq. (2) in Eq. (3), we obtains:

$$\frac{dE}{dx} \geq \frac{4\pi\gamma^2(T)}{3\eta(P_v - P_o)} \tag{4}$$

Equation (4) shows that if (dE/dx) is higher than $\left(\frac{4\pi\gamma^2(T)}{3\eta(P_v-P_o)}\right)$, the drop is completely evaporated and turns into a bubble. The stopping power on the left of (dE/dx) is related to neutron energy, whereas the expression on the right depends on thermodynamic parameters such as temperature and pressure. In Table 1, the physical parameters of Freon-12 are listed at ambient pressure ($P_o = 1atm$), where the efficiency factor is taken as $\eta = 4\%$.

When SED is exposed to thermal neutrons, due to the presence of Cl in the Freon-12 droplets and the Li in the gel medium, particles of the sulfur ion, proton, alpha, and tritium are emitted according to the following nuclear reactions.

$${}^6_3Li + {}^1_0n \rightarrow {}^3_1H + \alpha \;\; Q = 4.78\ MeV, E_\alpha = 2.05\ MeV, E_{{}^3_1H} = 2.73\ MeV$$

Table 1
Physical parameters of Freon-12 (CCl_2F_2) at 25 °C [20,21].

Parameter	Freon-12 (CCl_2F_2)
Temperature (T) [°C]	25
Density (ρ) [$g.cm^{-3}$]	1.311
Surface tension ($\gamma(T)$) [$dyn\ cm^{-1}$]	9.013
Vapor pressure (P_v) [atm]	6.43
Degree of superheated ($\Delta P = P_v - P_0$) [atm]	5.43
Critical radius ($r_c = 2\gamma(T)/\Delta P$) [$\mu m$]	0.0328
The minimum energy required to transform a microbubble into a visible bubble $\left(W = \frac{16\pi(\gamma(T))^3}{3(\Delta P)^2}\right)$ [keV]	0.253
Minimum energy required for bubble formation ($E_{min} = W/\eta$) [keV]	6.32
$\left(\frac{dE}{dx} \geq \frac{W}{2\eta R_c}\right)$ [$keV\ \mu m^{-1}$]	$dE/dx \geq 96.417$

$${}^{35}_{17}Cl + {}^1_0n \rightarrow {}^{35}_{16}S + p \;\; Q = 615\ keV, E_{{}^{35}_{16}S} = 17\ keV, E_p = 598\ keV$$

The resulting α-particle has a small range (around 13 μm). It is possible to calculate the energy deposited by an ion at a given distance based on its stopping power. Table 2 presents the stopping power and the range of charged particles from ${}^6_3Li$ and ${}^{35}_{17}Cl$ interactions in Freon-12 ($\rho = 1.311\ gcm^{-3}$ at 25°C) as calculated using the SRIM code [22].

The stopping power and range of each ion are different in SED. The sulfur ion deposits its energy in a range of 0.0463 μm which is less than 2 r_c ($= 0.0656\ \mu m$), while the proton cannot deposit sufficient energy to create a bubble in the critical radius. Since charged particles from neutron interactions with ${}^6_3Li$ have a long range, their presence in a gel medium can cause bubbles. Using the SRIM code, it was calculated that bubble formation can occur if an α-particle from ${}^6_3Li(n.\alpha){}^3_1H$ reaction is generated 10.16 μm away from the drop [22]. The allowed range for Li ions around a droplet is illustrated in Fig. 1. Thus, adding Li to the gel medium of an ordinary Freon-12 detector increases its sensitivity to thermal neutrons, making it suitable for detecting neutron energies from thermal to fast.

3. Material and methods

The experiments were performed with Freon-12 SED fabricated in the neutron laboratory of Amirkabir University of Technology. Detectors were prepared according to the method by Raisali et al. [23]. The density of the viscoelastic gel and Freon-12 liquid was adjusted with saturated CsCl and 3.4 % LiCl solutions mixed into a 35 % polyacrylamide solution. Then 3 ml of the mixture was transferred to the 13 × 100 mm screw cap test tube, and 0.01 ml of Ammonium Persulfate was added as the initiator. After degassing by a water aspirator, 0.01 ml of an activator, namely Tetramethylenediamine (TEMED), was added before being sealed, and then placed in a dry ice-ethanol bath. Due to Freon-12's low boiling point, a sufficient amount of this material must be injected into the frozen gel prior to polymerization. Using a shaker with a speed of 2,600 rpm, Freon-12 liquid was broken and dispersed in the gel. Also, additional amount of Freon-12 was added to pressurize the gel medium to deactivate SED against neutron radiation. To activate

Table 2
The stopping power and the range of charged particles in SED calculated by SRIM code.

Density: 1.311 g/cm^3	Freon-12 (CCl_2F_2)			
Reaction	${}^6_3Li(n.\alpha){}^3_1H$		${}^{35}_{17}Cl(n,p){}^{35}_{16}S$	
Products	${}^4_2He$	${}^3_1H$	${}^1_1H$	${}^{35}_{16}S$
Energy (MeV)	2.05	2.73	0.598	0.017
Range (μm)	13.36	76.53	14.89	0.0463
Stopping power (keV /μm)	139.2	24.02	28.01	42.98

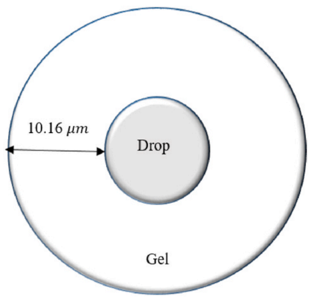

Fig. 1. A schematic drawing of the allowed range for Li ions around a droplet.

SED, excess Freon-12 was released and the temperature of SEDs got lower due to Freon-12 evaporation. After 1 h in the radiation room, the temperature of the detectors reached equilibrium with room temperature. Bubbles were formed in the detector when placed in the field of thermal neutrons from an Am–Be source. To reset the SEDs, they were frozen in a dry ice-ethanol bath and relocated to room-temperature water. This recompresses the bubbles back into liquid drops. To investigate the effect of Li in the fabricated SEDs, we simultaneously used it and an ordinary Freon-12 detector. The presence of Li in the SED makes it sensitive to thermal neutrons in addition to fast neutrons. After both detectors are simultaneously exposed to thermal neutrons, the difference in the number of formed bubbles indicates the sensitivity of the SED to thermal neutrons. The detectors were irradiated with an ^{241}Am–Be neutron source with 15 Ci activity (and neutron emission rate of 3.3×10^7 $(\mathrm{n\,s^{-1}})$) in the neutron laboratory at Amirkabir University of Technology. The source was encased in a cylindrical stainless-steel container with 4.02 cm in diameter and 13.72 cm in height at a temperature of 25 $^{\circ}C$. The Am–Be source was situated at the center of a cylindrical steel tank filled with water which has a height of 1.5 m and a radius of 77 cm in an iron casing. Iron cylinders were located in the water around the source at different distances from each other, as shown in Fig. 2. These cylinders were used to irradiate SEDs with thermal neutrons.

On the other hand, the thermal neutron flux in the desired location was determined using the Boron-lined proportional counter. The used Reuter-Stokes Boron-lined proportional counter (model RS-P7-0812-117) in this study has a sensitive length of 29.5 cm and a diameter of 2.5 cm. The inner wall of the volume is coated with 92%-enriched Boron

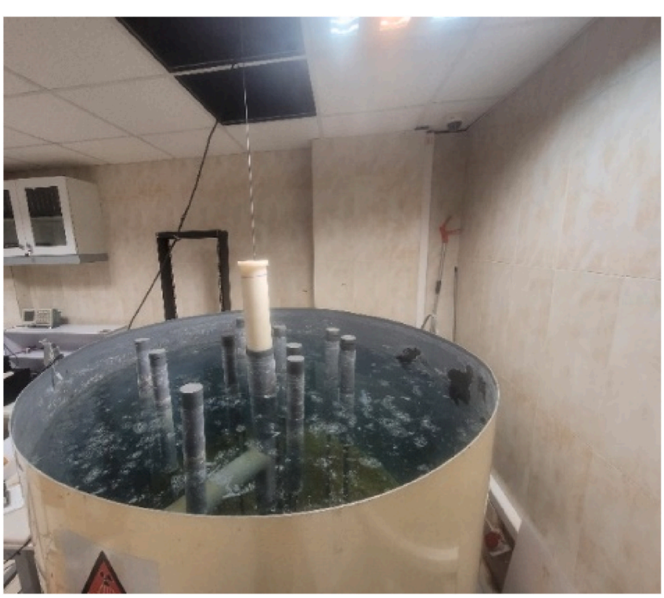

Fig. 2. Am–Be source is placed at the center of the iron tank containing water.

atoms, ^{10}B and filled with a mixture of Argon-CO_2 at a pressure of 0.262 atm. In order to validate thermal neutron flux, the MCNP simulation code based on the Monte Carlo method [24] was used. By designing and modeling the SED in the thermal neutron field, the average thermal neutron flux was calculated in a similar situation.

The sensitivity of the detector, expressed in bubbles/μSv, is determined using the following equation:

$$S = \frac{N}{H^{*}(10)} \tag{5}$$

where N represents the number of bubbles recorded by the detector when exposed to the ambient dose equivalent H*(10) [25].

The detector's sensitivity was determined utilizing the dose acquired from the MCNP code in the prepared set-ups, based on NCRP 38 recommendation.

4. Results and discussion

To irradiate SEDs, cylinders located 15 cm, 25 cm, 35 cm, and 45 cm from the source were chosen. Then a Freon-12 SED with Li and an ordinary Freon-12 SED were placed in each chosen cylinder. Next, they were exposed to thermal neutrons for 10, 15, and 20 min, respectively. After irradiation, small bubbles can be seen which can be counted by the naked eye. By comparing the number of formed bubbles in the two SEDs, the number of bubbles due to the presence of Li was determined. This means that the detector containing Li is more sensitive to thermal neutrons. The results of this experiment are shown in Table 3. The first and second rows of this table, represent the distance of SEDs from the source and the duration of irradiation respectively. The nucleation rate is calculated in the third row the ratio of the number of created bubbles to the irradiation time. Four SEDs were irradiated for each distance in order to minimize measurement uncertainty and avoid bubble overlap. Based on the Poisson statistics, the associated uncertainty of the average number of bubbles in the irradiated SEDs is determined as follows:

$$u = \sqrt{\overline{M}/n} \tag{6}$$

where $\overline{M}$ refers to the average number of formed bubbles and n is the number of irradiated detectors. Given the uncertainty caused by bubble determination, the normalized nucleation rate was presented in the last row of the table.

To enhance counting efficiency, the irradiation time was increased with the distance from the source. Accordingly, more bubbles formed due to the increase in thermal neutron interaction. Since the fast and thermal neutron fluxes vary for different water thicknesses it was observed that the number of formed bubbles decreased with the increase in the distance of SEDs from the source. Fig. 3 presents the nucleation rate diagram as a function of the SED's distance from the neutron source, based on the number of formed bubbles. By drawing a fitting curve, it was found that the decrease in the SED's response with respect to the distance from the neutron source is almost from order −2. As expected, it follows from this inverse square reduction that the response of the SED

Table 3
Nucleation rate caused by the presence of Li ions in SEDs irradiated by Am–Be source at room temperature.

Distance from source (cm)	15	25	35	45
Irradiation time (s)	600	900	1200	1200
Nucleation rate ($bubbles/s$)	0.111	0.027	0.014	0.012
Normalized nucleation rate ($bubbles/s$)	1.00 ± 0.048	0.24 ± 0.004	0.13 ± 0.001	0.11 ± 0.001

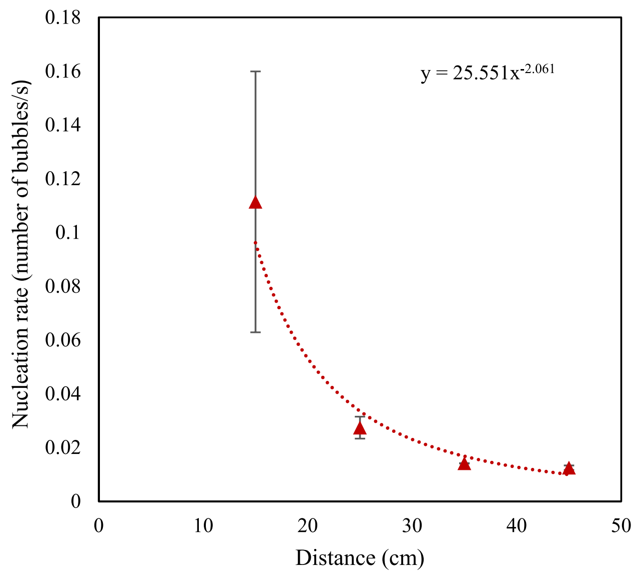

Fig. 3. Nucleation rate (bubbles/s) in SED as a function of distance from the source of Am–Be neutrons.

is proportional to the neutron flux. The detection sensitivity is defined as the ratio of the number of bubbles to the neutron flux [26]. As a confirmation, the thermal neutron flux at the prepared set-up is determined, and its relation with the response of SED is examined.

The Li-based fabricated SED was placed at a distance of 15 cm from the source for 10 min. Fig. 4 illustrates this detector before and after irradiation.

To estimate the thermal neutron flux at a specific position around the Am–Be source, experimental and simulation studies were conducted using a Boron-lined proportional counter and the MCNP code, respectively. Fig. 5 provides a schematic view of the position of the Am–Be source and the location at which the thermal neutron flux was measured.

A Boron-lined proportional counter was placed at 15, 25, 35, and 45 cm from the neutron source for 10, 15, and 20 min. Total neutron count was obtained and used to calculate the thermal neutron count rate as the ratio of neutron count to the duration of irradiation. Measurements were repeated three times for each location. Since the count rate is proportional to the thermal neutron flux, the last row of Table 4 refers to the

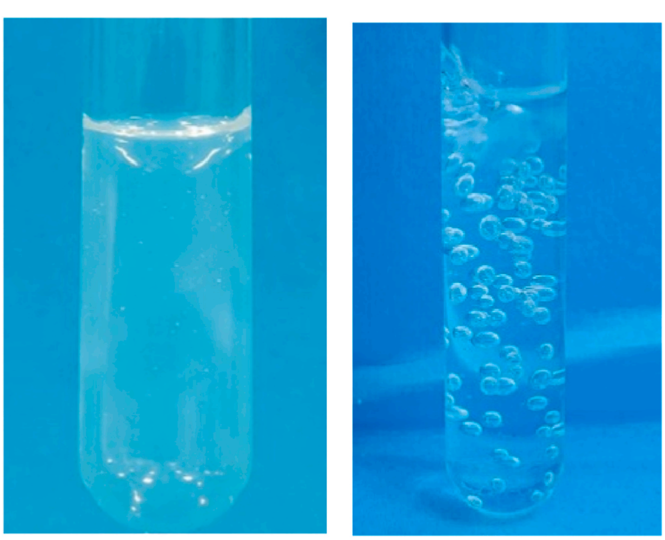

Fig. 4. Fabricated superheated emulsion detector before (left) and after irradiation (right).

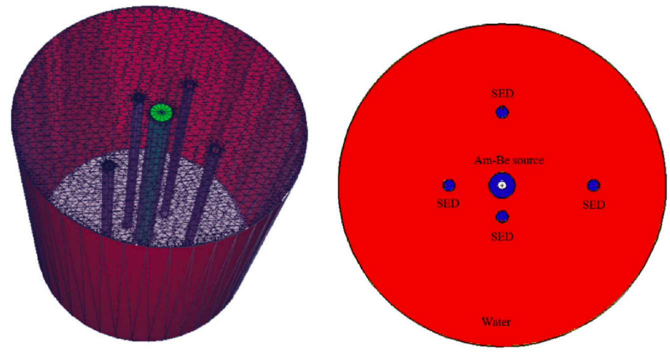

Fig. 5. Schematic view of the source, cylinders, and detector's location in Monte Carlo calculation.

Table 4
Calculated thermal neutron count rate using boron-lined proportional counter.

Distance (cm)	15	25	35	45
Time of irradiation (s)	600	900	1200	1200
Thermal neutron count rate (n/s)	2.00×10^4	0.47×10^4	0.09×10^4	0.03×10^4
Normalize thermal neutron flux	1 ± 0.50	0.23 ± 0.58	0.04 ± 0.58	0.01 ± 0.57

normalized relative thermal neutron flux.

Using MCNPX 2.7 code, the thermal neutron flux was benchmarked at selected set-ups by modeling the Am–Be neutron source, the SEDs, and the water tank. The average thermal neutron flux was then determined within the volume of SEDs at the desired location. The results are reported in Table 5.

Fig. 6 depicts the normalized thermal neutron flux obtained from simulation and experimental studies at specific distances from the Am–Be source. Good correspondence between results achieved from the two methods is observed.

Fig. 7 is a plot of the relation between the response of SED and the flux of thermal neutrons at each desired location. The results prove that the number of bubbles is linearly related to the thermal neutron flux as a function of $y = 0.0038x$ (y and x represent the number of bubbles and the thermal neutron flux respectively) with a correlation coefficient of 0.9935. Hence, the number of bubbles is indicative of the flux of thermal neutrons. Similar to an ordinary SED, the number of bubbles formed in a developed SED is directly proportional to the incident neutron flux, thereby serving as an indicator of the thermal neutron flux [26–29].

The thermal neutron dose at specific locations around the Am–Be source was determined using the MCNP code according to NCRP 38 recommendations. As demonstrated in Fig. 8, the number of bubbles forming in SED is linearly proportional to the dose.

According to equation (5), the sensitivity of SED was estimated as an average around 19 bubble/μSv. Various values for BDT sensitivity have been reported by other researchers as listed in Table 6. The manufacturer of BDT, in accordance with the NCRP 38 recommendations, expressed a sensitivity range of approximately 0.2–0.5 bubbles/μSv for thermal neutrons [30]. Due to the gel medium utilized in the SED, more bubbles were formed within the detector. Consequently, the lower sensitivity of BDT can be attributed to its firm polymer medium which

Table 5
Calculated thermal flux using MCNP code.

Distance (cm)	15	25	35	45
Thermal neutron flux $(\#/cm^2s)$	2.67×10^4	0.55×10^4	0.11×10^4	0.03×10^4
Normalized thermal neutron flux	1.00	0.20	0.04	0.01

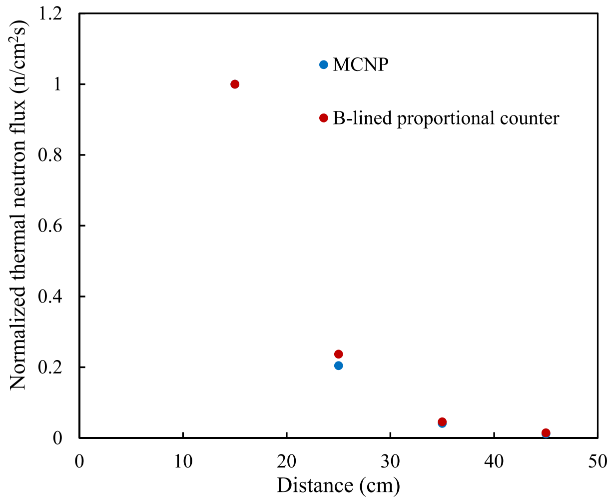

Fig. 6. Thermal neutron flux at 15, 25, 35, and 45 cm from Am–Be source.

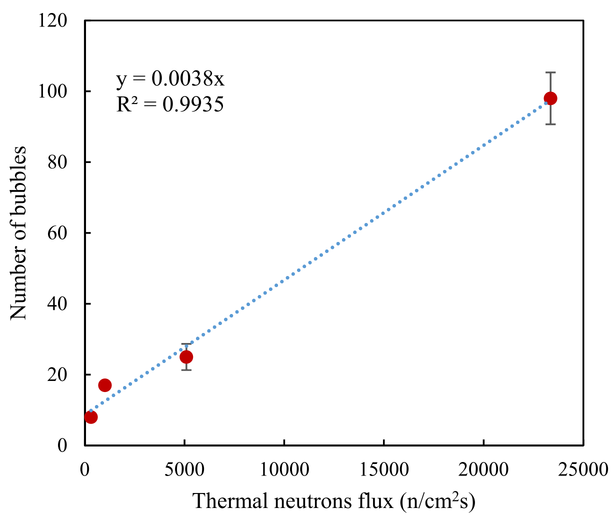

Fig. 7. Number of bubbles in SED as a function of thermal neutrons flux.

leads to fewer bubbles being formed.

5. Conclusion

A Freon-12 SED containing lithium was fabricated to be used as a suitable thermal neutron detector. A lithium compound was added to the host gel and the response of the SED was analyzed based on the thermal neutron flux at chosen set-ups around the Am–Be source. The flux of thermal neutrons was measured through simulation as well as using other detectors (i.e., Boron-lined detector). The results demonstrate that in comparison to ordinary SEDs, the sensitivity of a Li-containing SED to thermal neutrons significantly improved. Accordingly, it can be used as a neutron detector over a wide range of thermal to fast neutron energies. Also, it proved that the number of bubbles in the developed SED is proportional to the thermal neutron flux and dose received by the detector. Moreover, a higher sensitivity was observed for SED as compared to BDT which can be attributed to the gel medium utilized in SED as opposed to the firm polymer medium in BDT.

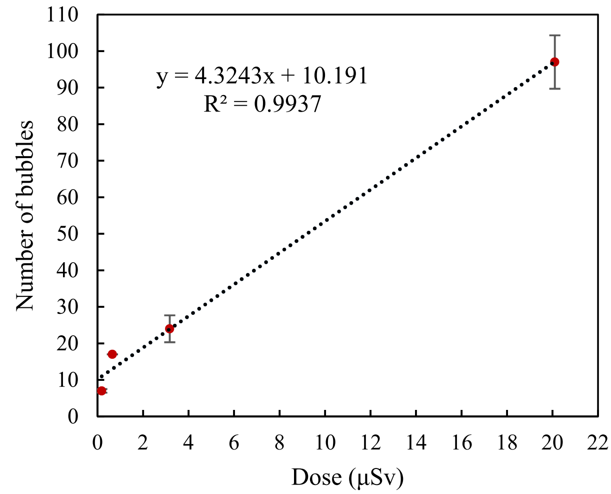

Fig. 8. Number of bubbles in SED as a function of dose equivalent.

Table 6
SED sensitivity compared to the reported values of BDT.

Sensitivity (bubbles/μSv)	Ref.
2.7	[11]
0.2–0.5	[30]
2–3	[31]
0.37–0.41	[25]
19 (average)	This work

Funding

This research did not receive any specific grant from funding agencies in the public, commercial, or not-for-profit sectors.

Declaration of competing interest

The authors declare that they have no known competing financial interests or personal relationships that could have appeared to influence the work reported in this paper.

Acknowledgments

The authors would like to thank Mr. Ali Elhampour, Mr. Soroush Mohtashami, and Mr. Mahdi Sahraian for their assistance during this research work. The authors are also thankful to the neutron laboratory at the Amirkabir University of Technology for providing the Am–Be source.

References

[1] R.L. Moss, Critical review, with an optimistic outlook, on boron neutron capture therapy (BNCT), Appl. Radiat. Isot. 88 (2014) 2–11.
[2] Matthew P. Blakeley, Paul Langan, Nobuo Niimura, Podjarny Alberto, Neutron crystallography: opportunities, challenges, and limitations, Curr. Opin. Struct. Biol. 18 (5) (2008) 593–600.
[3] Richard T. Kouzes, James H. Ely, Luke E. Erikson, Warnick J. Kernan, Azaree T. Lintereur, Edward R. Siciliano, Daniel L. Stephens, David C. Stromswold, Renee M. Van Ginhoven, Mitchell L. Woodring, Neutron detection alternatives to 3He for national security applications, Nucl. Instrum. Methods Phys. Res. Sect. A Accel. Spectrometers Detect. Assoc. Equip 623 (3) (2010) 1035–1045.
[4] A. Ravazzani, A.F. Para, R. Jaime, M. Looman, M.M. Ferrer, Characterisation of He-3 proportional counter, Radiat. Meas. 41 (5) (2006) 582–593.
[5] D.R. Ochbelagh, Comparison of 3He and BF3 neutron detectors used to detect hydrogenous material buried in soil, Radiat. Phys. Chem. 81 (4) (2012) 379–382.
[6] Alan J. Hurd, Richard T. Kouzes, Why new neutron detector materials must replace helium-3, Eur. Phys. J. A 129 (236) (2014) 3.
[7] D.A. Shea, D. Morgan, The helium-3 shortage: supply, demand, and options for congress, in: CRS Report for Congress, Congressional Research Service, 2010.

[8] R.E. Apfel, The superheated drop detector, Nucl. Instrum. Methods 162 (1–3) (1979) 603–608.
[9] H. Ing, H.C. Birnboim, A bubble-damage polymer detector for neutrons, Nucl. Tracks Radiat. Meas. 8 (1–4) (1984) 285–288.
[10] J. Schulze, W. Rosenstoke, H.L. Kronholz, Measuremants of fast neutrons by bubble detectors, Radiat. Protect. Dosim. 44 (1/4) (1992) 351–354.
[11] A. Di Fulvio, C. Domingo, M. De San Pedro, E. D'Agostino, M. Caresana, L. Tana, F. d'Errico, Superheated emulsions and track etch detectors for photoneutron measurements, Radiat. Meas. 57 (2013) 19–28.
[12] S.C. Roy, R.E. Apfel, Y.-C. Lo, Superheated drop detector: a potential tool in neutron research, Nucl. Instrum. Methods 255 (1–2) (1987) 199–206.
[13] R.E. Apfel, Photon-insensitive, thermal to fast neutron detector, Nucl. Instrum. Methods 179 (3) (1981) 615–616.
[14] S. Vaijapurkar, R. Paturkar, R. Raman, P. Bhatnagar, A. Pandya, S. Roy, A neutron sensor based on superheated droplets, Radiat. Meas. 23 (4) (1994) 753–755.
[15] B.J. Lewis, M.B. Smith, H. Ing, H.R. Andrews, R. Machrafi, L. Tomi, T.J. Matthews, L. Veloce, V. Shurshakov, I. Tchernykh, N. Khoshooniy, Review of bubble detector response charactristics and resultsfrom space, Radiat. Protect. Dosim. 150 (1) (2012) 1–21.
[16] L.K. Pan, C.-K.C. Wang, Superheated-liquid-droplet technique for measuring alpha decays in uranium solutions, Nucl. Instrum. Methods Phys. Res. 420 (1999) 345–355.
[17] S.G. Vaijapukar, R.T. Paturkar, Superheated liquid neutron sensor based on polymer matrix, Radiat. Meas. 24 (3) (1995) 309–313.
[18] F. Seitz, On the theory of the bubble chamber, Phys. Fuids 1 (1) (1958) 2.
[19] R.E. Apfel, S.C. Roy, Y.-C. Lo, Prediction of the minimum neutron energy to nucleate vapor bubble in superheated liquids, Phys. Rev. 31 (5) (1985) 3194–3198.
[20] W. Lim, C.K. Wang, Computational studies of neutron response function for a neutron spectrometer which uses Freon-12, -22, and -115 superheated liquids, Nucl. Instrum. Methods 335 (1–2) (1993) 243–247.
[21] E.I. du Pont de Nemours & Co., Thermodynamic properties of DuPont™ Freon® 12 (R-12) refrigerants [Online]. Available: http://joho.p.free.fr/EC/ENERGIE/_Ressources/FLUIDES%20Frigorig%C3%A8nes/Dupont%20de%20Nemours/www.dupont.com/suva/emea/pdf/thermo_freon12.pdf, 2005.
[22] James F. Ziegler, M.D. Zigler, J.P. Biersack, SRIM-The stopping and range of ions in matter, Nucl. Instrum. Methods B 268 (11–12) (2010) 1818–1823.
[23] P. Rezaeian, G. Raisali, A. Akhavan, H. Ghods, B. Hajizadeh, Development of a new pressure dependent threshold superheated drop detector for neutrons, Nucl. Instrum. Methods 776 (2015) 50–56.
[24] Laurie S. Waters, Gregg W. McKinney, Joe W. Durkee, Michael L. Fensin, John S. Hendricks, Michael R. James, Russell C. Johns, Denise B. Pelowitz, The MCNPX Monte Carlo radiation transport code, AIP Conf. Proc. 896 (1) (2007) 81.
[25] M. Chemtob, R. Dollo, C. Coquema, J. Chary, , et al.C. Ginisty, Essais de dosimètres neutrons à bulles, modèle BD 100 R-PND et modèle BDT, Radioprotection 30 (1) (1995) 61–78.
[26] Guiying Zhang, Bangfa Ni, Li Li, Peng Lv, Weizhi Tian, Zhiqiang Wang, Chunbao Zhang, Hailong Luo, Shunli Jiang, Pingsheng Wang, Donghui Huang, Cunxiong Liu, Caijin Xiao, Study on bubble detectors used as personal neutron dosimeters, Appl. Radiat. Isot. 69 (10) (2011) 1453–1458.
[27] S.G. Vaijapurkar, R.T. Paturkar, Superheated liquid neutron sensor based on polymer matrix, Radiat. Meas. 24 (3) (1995) 309–313.
[28] D. Ponraju, H. Krishnan, S. Viswanathan, R. Indira, Preliminary results on bubble detector as personal neutron dosimeter, Radiat. Protect. Dosim. 144 (1–4) (2011) 177–181.
[29] P. Priyada, R. Ramar, H. Krishnan, S. Viswanathan, Shivaramu, "Gamma photon techniques for detection of nucleation in superheated emulsion detectors for neutron dosimetry,", Radiat. Protect. Dosim. 158 (1) (2013) 100–106.
[30] F. Vanhavere, M. Coeck, R. Noulty, The BDT bubble neutron detector for personal dosimetry, in: European IRPA Congress 2002, 2002. Italy.
[31] M. Weinstein, B. Ben-Shachar, U. German, S. Merling, R. Srebr, Experimental data for some characteristics of the bubble neutron detectors, in: Conference of the Nuclear Societies in Israel, 2002.